Accepeted in Journal of Magnetism and Magnetic Materials (2007)
http://dx.doi.org/10.1016/j.jmmm.2007.10.025

Study on electro-magnetic properties of La substituted Ni-Cu-Zn ferrite synthesized by auto-combustion method

P.K. Roy, Bibhuti B. Nayak, J. Bera[1]
Department of Ceramic Engineering,
National Institute of Technology, Rourkela-769008, INDIA

Abstract

$(Ni_{0.25}Cu_{0.20}Zn_{0.55})La_xFe_{2-x}O_4$ ferrite with x =0.00, 0.025, 0.050 and 0.075 compositions were synthesized through nitrate-citrate auto-combustion method. Crystalline spinel ferrite phase with about 16-19 nm crystallite size was present in the as-burnt ferrite powder. These powders were calcined, compacted and sintered at 950°C for 4hours. Initial permeability, magnetic loss and AC resistivity of different compositions were measured in the frequency range from 10Hz to 10MHz. Saturation magnetization and hysteresis parameters were measured at room temperature with a maximum magnetic field of 10 kOe. Permeability and AC resistivity were found to increase and magnetic loss decreased with La substitution for Fe, up to x=0.025. Saturation magnetization and coercive field also increases up to that limit. The electromagnetic properties were found best in the ferrite composition of x=0.025 which would be better for more miniaturized multi layer chip inductor.

PACS: Ferrites; 75.50.G

Keywords: Ceramic; soft ferrite; La substitution; Ni-Cu-Zn ferrites; electromagnetic properties.

[1] Corresponding author. Tel.: +91-9437246159
Fax: +91-661-2472926
E-mail address: jbera@nitrkl.ac.in (J.Bera)

1. Introduction

The miniaturization trend of electronic devices results in the rapid development of surface mount devices (SMD) [1-2]. As one of the most important SMD, multilayer chip inductors (MLCI) become more and more miniaturized and integrated [3]. Ni-Cu-Zn ferrites are well established soft magnetic material for MLCI applications because of their relatively low sintering temperature, high permeability in the RF frequency region and high electrical resistivity [4-5]. The magnetic properties of the ferrite are highly sensitive to the technology parameters, especially to the amount of constituent metal oxides or additives in their compositions [6]. The magnetic properties can be changed by the substitution of various kinds of M^{+2} divalent cations (Co^{+2}, Mg^{+2}, Fe^{+2}, Mn^{+2}) or by introducing a relatively small amount of rare-earth ions [7]. Nowadays the rare earth oxides are becoming promising additives to improve the magnetic properties of ferrites [8, 9]. Many investigations have been carried out to understand the effect of La substitution on the properties of Ni-Zn ferrite [10-11], Mn-Zn ferrite [12], Mg-Cu ferrite [13], Ni-Cu-Zn ferrite [14]. Sun et al.[10] reported that the permeability of Ni-Zn ferrite decreased with La substitution and that has been interpreted by a combination of low density, small grain size, secondary phase $LaFeO_3$ formation and creation of more lattice defects. However, Ahmed et al. [12] reported an increase in susceptibility in Mn-Zn ferrite by the same substitution. Also an increase in permeability of Ni-Cu-Zn ferrite by the substitution has been reported recently [14]. Many investigators reported either decrease [8, 12] or increase [11, 13, 14] in resistivity and grain size of ferrites with rare earth addition. All these indicate that further detailed investigations are needed on this type of La-substitutions. Therefore, purpose of our investigation is to study the effect of La^{+3} substitutions for Fe^{+3} on the electromagnetic properties of Ni-Cu-Zn ferrite; such as permeability, magnetic loses, resistivity, saturation magnetization and hysteresis parameters. A significant improvement of electro-magnetic properties of this commercially important ferrite has been reported here.

2. Experimental

The ferrite powders were synthesized through nitrate-citrate auto combustion route to achieve homogeneous mixing of the chemical constituents on the atomic scale and better sinterability. Analytical grade of nickel nitrate [$Ni(NO_3)_2.6H_2O$], zinc nitrate [$Zn(NO_3)_2.\ 6H_2O$], copper nitrate [$Cu(NO_3)_2.3H_2O$], iron nitrate [$Fe(NO_3)_3.9H_2O$], citric acid [$C_6H_8O_7.H_2O$] and lanthanum nitrate [$La(NO_3)_3$] were used to prepare $(Ni_{0.25}Cu_{0.20}Zn_{0.55})La_xFe_{2-x}O_4$ ferrite with x =0.00,

0.025, 0.050 and 0.075 compositions . Metal nitrates and citric acid were dissolved in deionized water. Metal nitrate solutions were standardized by chemical analysis and required amount of nitrate solutions were mixed with citric acid solution in 1:1 molar ratio of nitrates to citric acid. The pH of the solution was adjusted to 7 using ammonia. The solution was first heated at 80ºC to transform into gel and then ignited in a self-propagating combustion manner to form a fluffy loose powder. The as-burnt ferrite powders were then calcined at 700^{o}C for 2h. The calcined powders were granulated using PVA as a binder and was uniaxially pressed at a pressure of 275 MPa to form toroidal and pallet specimens. The specimens were sintered at 900^{o}C for 4hr in air. The ferrites were characterized by X-ray diffraction (PW-1830, Philips, Netherlands) using Cu-Kα radiation. The crystallite size was calculated from X-ray peak broadening of the (311) peak using Scherrer formula. Microstructure of the sintered specimens was analyzed by SEM (JSM 6480 LV JEOL, Japan). Impendence analyzer (Hewlett Packard, Model 4192A, USA) was used to measure inductance on toroids, wound with low capacitive 6 turns enameled copper wire. Resistivity was measured on pallet samples, by applying silver electrodes on the surfaces using $\rho=1/(\omega\epsilon_0 k' \tan\delta)$ formula. Saturation magnetization and hysteresis parameters were measured at room temperature using a vibrating sample magnetometer (VSM) (Lakeshore-7040) with a maximum magnetic field of 20 kOe.

3. Results & Discussion

Fig.1 and 2 show the XRD patterns of the as-burnt and sintered ferrite respectively. As-burnt powder contains crystalline spinel ferrite phases (JCPDS card No. 08-0234). The broad peaks in XRD patterns indicate fine crystallite size of the ferrite. The crystallite size of the as-burnt ferrite was found to be in the range of 16-19 nm. Though $LaFeO_3$ peak was not detected in all as-burnt powders (see Fig. 1) but this phase was detected in all sintered pellets (see Fig. 2). It has been established that the secondary phase $LaFeO_3$ was formed upon La substitution for Fe in the ferrite. The peak height of $LaFeO_3$ gradually increases with the substitution of La as seen from Fig. 2. A detailed study on this phase formation behavior has been described in our previous work [14].

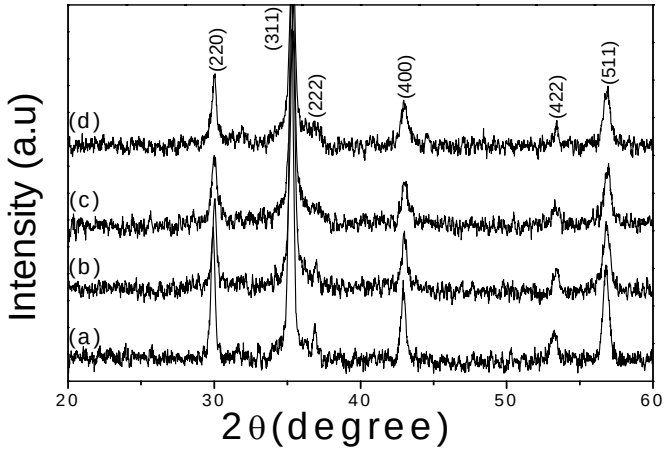

Fig.1 XRD patterns of the as-burnt $(Ni_{0.25}Cu_{0.20}Zn_{0.55})La_xFe_{2-x}O_4$ ferrite with (a)x =0.00, (b) x=0.025, (c) x=0.050, (d) x=0.075.

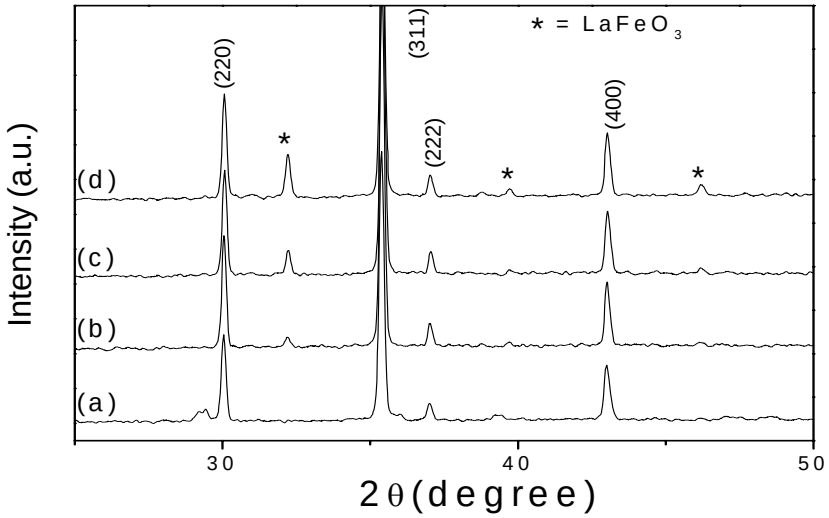

Fig.2 XRD patterns of the sintered $(Ni_{0.25}Cu_{0.20}Zn_{0.55})La_xFe_{2-x}O_4$ ferrite with (a)x =0.00, (b) x=0.025, (c) x=0.050, (d) x=0.075.

Fig. 3 shows the SEM microstructure of the sintered ferrites with different La substitutions. The undoped ferrite (Fig. 3A) shows a monophasic microstructure with about 0.6 μm grain size. However, all La-doped samples (Fig. 3 B, C and D) show a bi-phasic microstructure with bigger matrix grain and smaller grain at the grain boundary. The bigger grains are ferrite and smaller grains at boundary are $LaFeO_3$ [14]. The grain size of matrix ferrite phase increases with the increase in La-substitution. Similarly densification also increases with La-substitution. The bulk density and grain size data are given in Table 1. The grain size of ferrite phase was calculated using line intercept method.

Fig. 4 shows the frequency dependency of permeability in different compositions. The initial permeability significantly increases for x=0.025 composition compare to undoped sample which may be due to better densification, bigger grain size (see Table 1), decreased anisotropy [14]. The permeability of x=0.050 & 0.075 compositions are lower than x=0.025 composition mainly due to the presence of higher quantity of nonmagnetic $LaFeO_3$ phase. The permeability of x=0.025 composition is stable in the frequency range 100 kHz to 2MHz and its dispersion occurs above 2MHz. The dispersions of the other compositions are at higher frequency compared to x=0.025 composition. The dispersion behavior can be explained by Snoek's law that cut-off frequency is inversely proportional with magnetic permeability [15]. As we know the permeability and resonance frequency are not independent, but are related by $\mu_o^2\omega_x$ = constant [16]. So, lowest cut-off frequency of x=0.025 composition is due to its highest permeability among all.

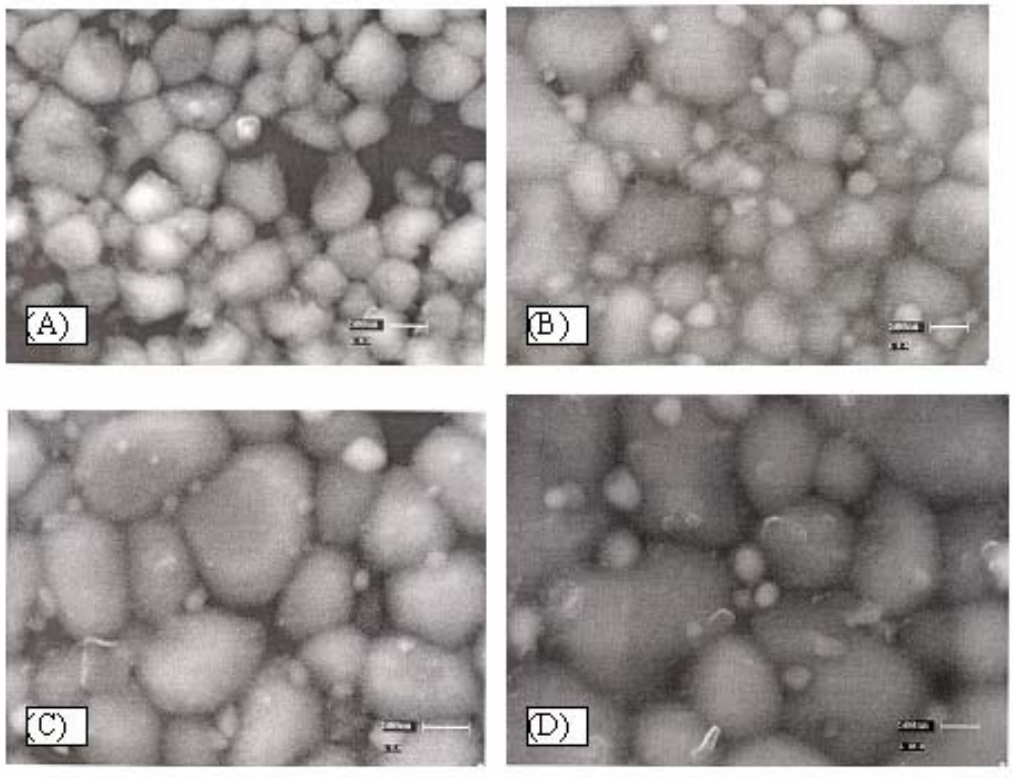

Fig. 3 SEM micrographs of sintered $Ni_{0.25}Cu_{0.20}Zn_{0.55}La_xFe_{2-x}O_4$ ferrite with (A)x =0.00, (B) x=0.025, (C) x=0.050, (D) x=0.075. The white bar indicates 500 nm.

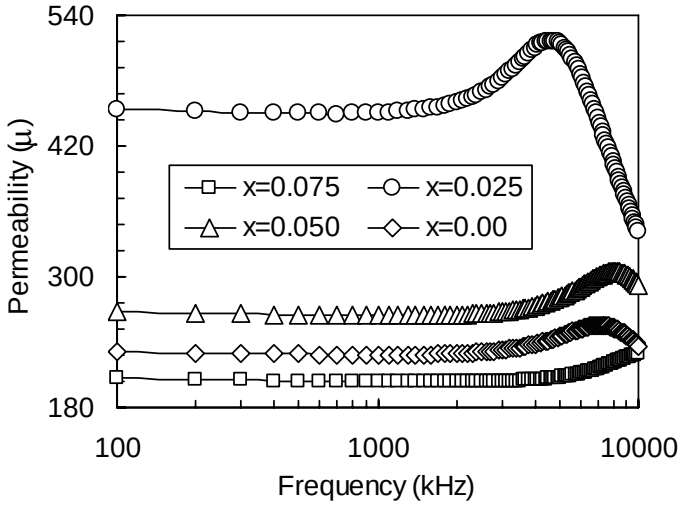

Fig. 4 Frequency dependency of permeability in $(Ni_{0.25}Cu_{0.20}Zn_{0.55})La_xFe_{2-x}O_4$ ferrites with different La (x) content.

Fig. 5 shows the magnetic Hysteresis curve for $(Ni_{0.25}Cu_{0.20}Zn_{0.55})La_xFe_{2-x}O_4$ ferrites. The saturation magnetization (*M*s) and coercive field (H_c) values of different compositions are given in Table 1. The saturation magnetization of composition x=0.025 is higher than undoped one. This may be due to better density and higher permeability of the doped ferrite. *M*s of x=0.050 & 0.075 compositions are lower than x=0.025 composition. This may be due to the presence of higher quantity of nonmagnetic $LaFeO_3$ in x=0.050 & 0.075 compositions. The two main magnetization mechanisms are wall displacement and spin rotation. The values of rotational permeability (μ_{rk}) have been calculated as per [17] using;

$$\mu_{rk} = 1+\frac{8\pi Ms}{3Ha} \qquad (1)$$

and the anisotropy field (*Ha*) is calculated as per [18] using;

$$Ha = 2K_1/ Ms \qquad (2)$$

Where, *M*s is the saturation magnetization, K_1 is the anisotropy constant which is taken as $-K_1 = 2.70*10^4$ erg/cm^3 [19] for all the compositions, considering no La solubility in the spinel ferrite structure. The calculated values of rotational permeability (μ_{rk}), wall permeability (μ_w) and anisotropy field (*Ha*) for different compositions are given in Table 1. It is evident from the table 1 that the magnitude of wall permeabilities are larger in compare to rotational permeabilities. So, wall permeability dominates the magnetization mechanism.

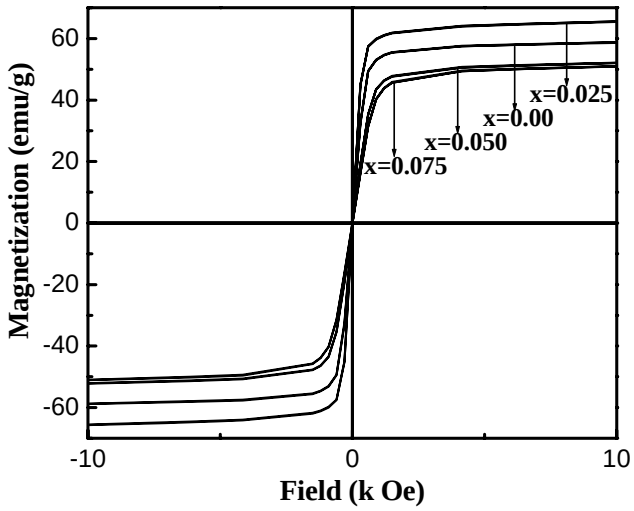

Fig. 5 Magnetic hysteresis curve for $(Ni_{0.25}Cu_{0.20}Zn_{0.55})La_xFe_{2-x}O_4$ ferrites with different La (x) content measured at room temperature.

Table 1 Saturation magnetization (*Ms*), wall permeability (μ_w), rotational permeability (μ_{rk}), coercive field (*Hc*), anisotropy field (*Ha*) and resistivity (ρ) of $(Ni_{0.25}Cu_{0.20}Zn_{0.55})La_xFe_{2-x}O_4$ ferrite with different x values.

Composition	Bulk density (g/cm^3)	Grain size (μm)	*Ms* (emu/cm^3)	μ_w	μ_{rk}	*Hc* (Oe)	*Ha* (Oe)	Resistivity (ohm-cm)
x=0.00	4.6	0.6	273.19	189.42	12.58	0.74	197.60	$0.39*10^7$
x=0.025	4.9	0.86	321.89	406.93	17.07	2.22	167.76	$0.69*10^8$
x=0.050	5.0	0.95	266.18	234.01	11.99	0.51	202.80	$0.61*10^8$
x=0.075	5.1	1.2	263.64	177.21	11.79	0.45	204.76	$0.42*10^8$

All compositions exhibit low coercivity values, which is typical of soft ferrite. Coercivity increased in x=0.025 composition compared to undoped sample, which may be due to an extrinsic effect associated with a favorable microstructure in the sample [20]. Since coercivity is the micro-structural property, it depends upon defects, strains, non-magnetic atoms etc. in the material. However, the coercivity (H_c) decreases with further La addition. This may be due to the higher grain size (see Table 1) in later two compositions, as we know *H*c decreases with increasing grain size.

Electrical resistivity is an important property of low temperature sintered ferrite for MLCI application. The AC resistivity (ρ) was calculated using the formula:

$$\rho = 1/ (\omega \epsilon_0 k' \tan\delta) \qquad (3)$$

Where, ϵ_0 is the permittivity of free space, k′ is the relative dielectric constant, tanδ is dissipation factor, ω is the angular frequency. Resistivity of the ferrite (see Table 1) increases with increase in La content with respect to undoped ferrite. It is well known that the magnetic anisotropy field in ferrites results mainly from the presence of Fe^{+2} ions [21]. The anisotropy field (see Table 1) for x=0.025 composition is lower than the undoped sample, i.e Fe^{+2} ion concentration is lower for this composition. That's why the x=0.025 composition has higher resistivity compared to undoped ferrite. Decreased Fe^{+2} ionic concentrations may be attributed due to the formation of secondary $LaFeO_3$ phases. The crystallization of $LaFeO_3$ phase on the grain boundaries impedes the oxidation of Fe^{+3} ions inside the grains during cooling of the samples. A small decrease in resistivity in x=0.05 and 0.075 compositions may be due to the increase in grain size (see Table 1). As we know, larger grains result in less no of grain boundaries, which act as scattering center for the flow of electrons and therefore decrease of resistivity.

Fig. 6 shows the relative loss factor (RLF) i.e. the ratio of the magnetic loss tangent to initial permeability of different cores. High μ and low tanδ i.e. low RLF is required for high frequency magnetic applications. It is revealed from the Fig. that the RLF of La-substituted ferrites are lower than undoped one upto 2 MHz. The predominant losses in ferrite are due to hysteresis and eddy current losses at operating frequency lower than the relaxation frequency of wall displacement. The hysteresis loss depends on many parameters like magnetostriction constant, magneto-crystalline anisotropy, saturation magnetization and microstructure. The eddy current loss mainly depends on the electrical resistivity of the ferrite. So, it may be consider that the lowering of RLF in La-substituted compositions resulted mainly from a reduction in eddy current loss due to their higher electrical resistivity. The RLF of all the cores increased in MHz frequency zone due to the resonance-relaxation losses. The undoped ferrite shows highest RLF in 100 to 1000 kHz zone. This may be due to its higher porosity and lower resistivity [14, 22]. The x=0.025 composition has lowest RLF up to 2 MHz and hence the best material for MLCI applications.

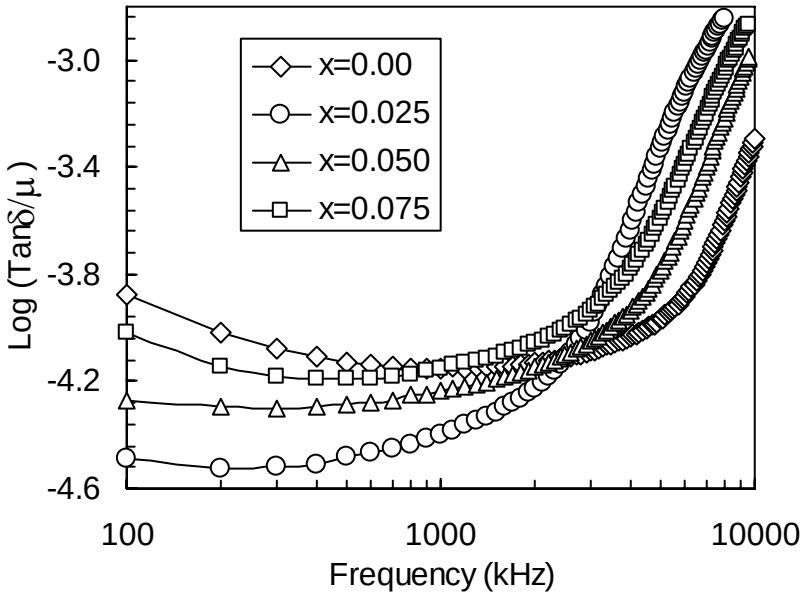

Fig. 6 Relative loss factor as a function of frequency in $(Ni_{0.25}Cu_{0.20}Zn_{0.55})La_xFe_{2-x}O_4$ ferrites with different La (x) content.

4. Conclusions

The effect of La substitution on electromagnetic properties in $(Ni_{0.25}Cu_{0.20}Zn_{0.55})La_xFe_{2-x}O_4$ ferrite has been investigated. Initial permeability and saturation magnetization were increased significantly at a small fraction of La (x=0.025) substitution. This may be primarily due to better densification of that substituted ferrite. The AC resistivity of the composition was also increased due to the lowering of Fe^{+2} ion concentration by the formation of $LaFeO_3$ phase at the grain boundary. The relative loss factor of the specific composition was lower due to the higher electrical resistivity as well as higher initial permeability. The magnetic loss of the composition was within a narrow limit in the frequency range 100 kHz to 2 MHz. So, the composition $(Ni_{0.25}Cu_{0.20}Zn_{0.55})La_{0.025}Fe_{1.975}O_4$ would be a better material for reducing the number of layers in MLCI and realizing more miniaturization.

Acknowledgement

Author, J. Bera wishes to thank the Department of Science & Technology, Govt. of India, New Delhi, for providing financial support through project grant (Grant no. SR/S3/ME/04/2002-SERC-Engg).

References

[1] I. Z. Rahman, T. T. Ahmed, J. Magn. Magn. Mater. 290-291 (2005) 1576.

[2] C. W. Kim, J. G. Koh, J. Magn. Magn. Mater. 257 (2003) 355.

[3] B. Li, Z. X. Yue, X. W. Qi, J. Zhou, Z. L. Gui, L. T. Li, Mater. Sci. Engg. B 99 (2003) 252.

[4] K. O. Low, F. R. Sale, J. Magn. Magn. Mater. 246 (2002) 30-35.

[5] H. I. Hsiang, W. C. Liao, Y. J. Wang, Y. F. Cheng, J. Euro. Ceram. Soc. 24 (2004) 2015–2021.

[6] O. F. Caltum, L. Spinu, Al. Stancu, L. D. Thung, W. Zhou, J. Magn. Magn. Mater. 242-245 (2002) 160.

[7] L. Zhao, Y. Cui, H. Yang, L. Yu, W. Jin, S. Feng, Mater. Lett. 60 (2006) 104-108.

[8] E. Rezlescu, N. Rezlescu, P. D. Popa, L. Reslescu, C. Pasnicu, Phys. Status Solidi, A 162 (1997) 673-678.

[9] L. Zhao, H. Yang, L. Yu, Y. Cui, X. Zhao, S. Feng, J. Magn. Magn. Mater. 305 (2006) 91-94.

[10] J. Sun, J. Li, G. Sun, J. Magn. Magn. Mater. 250 (2002) 20-24.

[11] M. A. Ahmed, E. Ateia, L. M. Salah, A. A. El-Gamal, Mater. Chem. Phys. 92 (2005) 310-321.

[12] M. A. Ahmed, N. Okasha, M. M. El-Sayed, Ceramics International, 33, 1 (2007) 49-58.

[13] E. Rezlescu, N. Rezlescu, P. D. Popa, J. Magn. Magn. Mater. 290-291 (2005) 1001-1004.

[14] P. K. Roy, J. Bera, Mater. Res. Bull. 42 (2007) 77-83.

[15] Y. Bai, J. Shou, Z. GUi, Z. YUe, L. Li, J. Magn. Magn. Mater. 264 (2003) 44-49.

[16] R. Valenzuela, in: Magnetic Ceramics, National University of Maxico, 1994.

[17] J. Smit, H. P. J. Wijn, Ferites, (John Wiley & Sons, New York, 1959)

[18] B. D. Cullity, Introduction of Magnetic Materials (Addision-Wesley Publishing Company, Indiana, 1972)

[19] S. A. Ghodake, U. R. Ghodake, S. R. Sawant, S. S. Suryavanshi, J. Magn. Magn. Mater. 305 (2006) 110-119.

[20] J. F. Wang, C. B. Ponton, R. Grossinger, I. R. Harris, J. Alloys Compds. 369 (2004) 170-177.

[21] E. W. Gorter, Philips Res. Rep. 9 (1954) 295.

[22] L. Neel, Physica, 15 (1949) 225-234.